Magnetic field rotation and transition width in rotational discontinuities and Alfvén wave trains

Y. Lin

Physics Department, Auburn University, Auburn, Alabama

L. C. Lee

Department of Physics, National Cheng Kung University, Tainan, Taiwan

Abstract. A hybrid simulation is carried out to study the evolution of magnetic field rotations in rotational discontinuities (RDs) and large-amplitude Alfvén wave trains (AWTs) whose initial field rotation angle $|\Delta\Phi| > 180°$. For a given initial half width D, the RDs or AWTs lose a multiple of $\pm 360°$ field rotation at a critical time, until a smallest rotation angle $|\Delta\Phi| < 180°$ is reached. The critical time t_c for losing the first $360°$ field rotation is found to be $t_c \simeq F(\Delta\Phi, \beta_1, \theta_{Bn})D^{3.3\pm0.8}$, where the function F decreases linearly with $\Delta\Phi$, decreases linearly with $\sqrt{\beta_1}$ for upstream ion beta $\beta_1 > 0.1$, and decreases with decreasing shock normal angle θ_{Bn}. At $t < t_c$, however, the rotation angle $\Delta\Phi$ remains unchanged. A search is conducted for minimum widths required for RDs to preserve their $|\Delta\Phi| > 180°$ for a given transient convection time at the dayside magnetopause and minimum widths of AWTs per $360°$ field rotation in the solar wind.

1. Introduction

Rotational discontinuities (RDs) and large-amplitude Alfvén waves have frequently been observed in the solar wind [*Burlaga*, 1971; *Lepping and Behannon*, 1980; *Neugebauer et al.*, 1984; *Alexander et al.*, 1987; *Neugebauer*, 1989, 1992, and references therein]. The thickness of the rotational discontinuities is found to be about a few to $\sim 10L_i$, where $L_i = c/\omega_{pi}$ is the ion inertial length [e.g., *Lepping and Behannon*, 1986]. Alfvén wave trains (AWTs) have also been observed in the solar wind [*Tsurutani and Gonzalez*, 1987; *Tsurutani et al.*, 1994]; some are high-intensity and long-duration (wavelengths of approximately tens of earth radii) and may be the cause of continuous aurora activities. The RDs have also been found at the Earth's magnetopause, where they play a very important role in the entry of solar wind plasma into the magnetosphere during magnetic reconnection events [*Sonnerup et al.*, 1981; *Berchem and Russell*, 1982; *Rijnbeek et al.*, 1988; *Scudder*, 1997].

In the MHD theory, in a plasma with an isotropic temperature the density, pressure, and magnetic field strength are conserved across an RD, while the tangential magnetic field changes its direction [*Landau and Lifshitz*, 1960]. The normal component of plasma flow

velocity upstream and downstream of the RD equals the local intermediate mode speed C_I, where $C_I = V_{An}$ and V_{An} is the normal component of the Alfvén velocity. While the ideal MHD does not give the internal structure of RDs, the structure of the RDs has been studied by including the dissipation and/or dispersion terms. A simple dissipative term in the MHD equations, however, results in a disintegration of RDs because of the conservation of entropy upstream and downstream of RDs. The structure of RDs has also been studied analytically on the bases of first-order orbit theory [*Su and Sonnerup*, 1968] and a time-independent kinetic model [*Lee and Kan*, 1982; *Wang and Sonnerup*, 1984]. These studies have shown the importance of trapped ion and electron particles in the formation of RD. The structure of nonlinear Alfvén waves and solitons has been studied by using two-fluid theories [*Sakai and Sonnerup*, 1983; *Buti*, 1988; *Kennel et al.*, 1988; *Hada et al.*, 1989; *Lyu and Kan*, 1989; *Hau and Sonnerup*, 1991].

Since the thicknesses of rotational discontinuities in the solar wind and at the magnetopause are of the order of several ion gyroradii, hybrid simulations have been used to study the structure of RDs in collisonless plasma. In the hybrid simulation, ions are considered to be particles, while electrons are considered to be a fluid. The ions, the electron fluid, and the electromagnetic fields evolve with time self-consistently. The existence of stable structures of RDs in one-dimensional (1-D) hybrid simulations has been reported by many authors [*Swift and Lee*, 1983; *Richter and Scholer*, 1989, 1991; *Lee et al.*, 1989; *Goodrich and Cargill*, 1991; *Krauss-Varban*, 1993; *Lin and Lee*, 1993; *Vasquez and Cargill*,

1993]. Each of these papers has discussed the RDs with certain shock normal angles θ_{Bn} between the upstream magnetic field and the direction normal to the shock front, values of upstream ion plasma β, rotation angle $\Delta\Phi$ of tangential magnetic field across the RDs, and the half widths D of the RD transition in units of the upstream ion inertial length L_i. Note that in the following, $\Delta\Phi > 0$ (< 0) denotes a right-handed or ion sense (left-handed or electron sense) rotation around the normal component of magnetic field.

Swift and Lee [1983] presented the first hybrid simulation of RDs. They showed that stable RDs exist for ion sense or electron sense field rotations. They also showed that the RDs with an initial field rotation angle $> 180°$ may be unstable. For example, an RD with $\Delta\Phi = \pm270°$ will turn into a new RD with a reversed-sense rotation of $\Delta\Phi = \mp90°$. They, however, did not discuss the dependence of their results on the thickness of RDs. *Lee et al.* [1989] conducted a study for the stability of RDs and intermediate shocks with $\theta_{Bn} = 60°$ and with various structures of initial transition region. The RDs were found to have a stable structure. A further investigation for RDs with $\theta_{Bn} < 45°$ was conducted by *Richter and Scholer* [1989]. They found that for small θ_{Bn} the RD tends to disintegrate into waves. *Goodrich and Cargill* [1991] showed, however, that the RDs with $\theta_{Bn} = 30°$ were also stable provided that the simulations were run for a long enough time. The waves developed at RDs are part of the RDs, and the RD may consist of a right-handed field rotation upstream and a left-handed field rotation downstream because of the polarizations of dispersive intermediate waves. The right-handed dispersive wave propagates faster than the MHD intermediate mode, while the left-handed wave propagates with a slower speed. The minimum shock width increases as θ_{Bn} decreases. The stability of RDs with small θ_{Bn} was further investigated by *Vasquez and Cargill* [1993]. On the basis of simulations of RDs with small ion β, *Vasquez and Cargill* [1993] examined the evolution of RDs with various θ_{Bn}, plasma beta, and the ion to electron temperature ratio T_i/T_e. The structure of RDs was explained in terms of linear and non-linear dispersive waves and ion kinetics associated with RDs. They found that the ion cyclotron mode waves produced from the RD are dispersive, leading to an expansion of the transition width. Note that phase standing occurs at large-θ_{Bn} RDs, where ion kinetics can damp dispersive modes [e.g., *Krauss-Varban*, 1993]. A recent simulation study by *Vasquez and Hollweg* [1998b] showed that stable RDs with small θ_{Bn} can be produced when the upstream and downstream conditions are relaxed, as they are in the Alfvén wave train, where the fields continue to rotate outside the RD layer. While the above simulations were for isolated RDs, the formation and structure of stable rotational discontinuities in the reconnection layer at the Earth's magnetopause were shown by *Lin and Lee* [1993].

Hybrid simulations also suggested that RDs with a magnetic field rotation angle $\Delta\Phi > 180°$ may exist for a long time if their transition width is wide enough. *Krauss-Varban* [1993] studied the relations between the structure and length scales of the RDs with $\theta_{Bn} = 60°$. It was found that there is a minimum thickness of a few L_i for transitions of both the ion and electron senses of field rotation. For $|\Delta\Phi| = 270° > 180°$ the RDs are unstable or metastable, but their breakup time increases with the initial thickness of the RD. The disintegration mechanisms are very different for the ion sense and the electron sense RDs with $|\Delta\Phi| = 270°$ [see also *Richter and Scholer*, 1991; *Goodrich and Cargill*, 1991].

Satellite observations at the magnetopause reported by *Berchem and Russell* [1982] showed that the magnetic field rotates from the magnetosheath direction to the magnetospheric direction by the shortest angular path. On the other hand, observations by *Sonnerup and Cahill* [1968] indicated that the direction of the magnetic field rotation across the magnetopause may depend on the normal component of the field and is in opposite sense above and below the magnetic equator. While most of the magnetopause crossings of satellites showed that magnetic field rotation follows the shortest path through RDs, a large field rotation of about $195°$ appeared in the RD observed by a magnetopause crossing of Ogo 5 [*Sonnerup and Ledley*, 1979]. An example of $\Delta\Phi > 270°$ was also found at the Uranian magnetopause [*Russell et al.*, 1989].

In our recent global hybrid simulation of the reconnection layer at the Earth's magnetopause, which is to be published elsewhere, magnetic field rotation angles of $|\Delta\Phi| > 180°$ were found in the RDs formed in the magnetopause current layer. This result and the observations of rotational discontinuities with $\Delta\Phi > 180°$ at the magnetopause motivated us to conduct a search for the structure of RDs with various angles $|\Delta\Phi| > 180°$ and with various initial thickness. One-dimensional hybrid simulations are used in our study. Since the sense of the rotation angle $\Delta\Phi$ through the magnetopause rotational discontinuity determines directly the sense of the field-aligned currents generated at the magnetopause current layer [e.g., *Lee et al.*, 1985; *Lin and Lee*, 1994], our present study is also very important for understanding the generation of field-aligned currents associated with the dayside magnetic reconnection and their roles in the generation of cusp field-aligned currents and dayside aurora.

A major purpose of this paper is to investigate the conditions for the existence of magnetic field rotations $|\Delta\Phi| > 180°$ in rotational discontinuities and Alfvén wave trains. The outline of the paper is as follows. The simulation model is presented in section 2. The simulation results of the evolution of RDs and AWTs are shown in section 3. A parameter search for cases with various shock normal angle θ_{Bn}, ion plasma β, field rotation angle $\Delta\Phi$, and initial thickness D is shown in

section 4. Applications of the results to the magnetopause and the solar wind are discussed. Finally, a summary is give in section 5.

2. Model of the Study

The 1-D hybrid code used in this study is the one described by *Swift and Lee* [1983]. In the hybrid model, ions are treated as discrete particles moving in a self-consistent electromagnetic field, and electrons are treated as a massless fluid. Charge neutrality is assumed in calculations. In the 1-D system, all the physical quantities are functions of position z and time t, while the magnetic field and flow vectors may have three components.

The initial profile in our simulation includes a finite transition region linking two uniform regions determined by the Rankine-Hugoniot conditions of rotational discontinuities. The normal of the RD front is in the z direction. The normal component of magnetic field $B_n = B_z = $ const in the 1-D system, which is assumed to be positive. An isotropic ion temperature is assumed initially at $t = 0$. A zero electron temperature $T_e = 0$ is assumed for simplicity. Note that in the magnetosphere, T_e is usually much less than the ion temperature.

In this paper, we name the cases with $|\Delta\Phi| \geq 360°$ Alfvén wave trains. The initial setup of AWTs is similar to that of the RDs. The initial RD or AWT is located at $z = 0$, and the upstream (downstream) region of the RD or AWT is located in $z > 0$ ($z < 0$). Let the subscripts "1" and "2" represent the quantities in upstream and downstream, respectively. The x and y components of magnetic field in the initial RDs or large-amplitude Alfvén wave trains are given as

$$B_x(z) = B\cos\Phi(z) \qquad (1)$$

$$B_y(z) = B\sin\Phi(z), \qquad (2)$$

where the magnetic field strength

$$B(z) = B_1 = B_2 \qquad (3)$$

and the azimuthal angle of the magnetic field

$$\Phi(z) = 0.5(\Phi_1 + \Phi_2) + 0.5(\Phi_1 - \Phi_2)\tanh(z/D). \qquad (4)$$

Here, D denotes the half width of the initial RD or AWT. The upstream magnetic field is assumed to be in the x direction, with $\Phi_1 = 0°$. The total field rotation angle across the RD or AWT can be written as $\Delta\Phi = (\Phi_2 - \Phi_1) > 0$ ($\Delta\Phi < 0$) for a right-handed or electron sense (left-handed or ion sense) rotation. The ion temperature and ion number density at the initial RD are given as

$$T(z) = T_1 = T_2 = \text{const} \qquad (5)$$

$$N(z) = N_1 = N_2 = \text{const}, \qquad (6)$$

respectively. The simulation is conducted in the frame that is comoving with the RD. The normal component of the flow velocity is equal to the intermediate mode speed, which is given by

$$V_z(z) = -B_n/\sqrt{\mu_0 m_i N(z)} = V_{z1} = V_{z2}, \qquad (7)$$

where m_i is the ion mass. The upstream and downstream tangential flow velocities are assumed to be field-aligned, with $(V_{x1}, V_{y1}) = (V_{Ax1}, V_{Ay1})$ and $(V_{x2}, V_{y2}) = (V_{Ax2}, V_{Ay2})$. The tangential flow velocity is assumed to satisfy MHD Walen relation everywhere in the RD, which can be written as

$$V_x(z) = V_{x1} - (B_x(z) - B_{x1})/\sqrt{\mu_0 m_i N(z)} \qquad (8)$$

$$V_y(z) = V_{y1} - (B_y(z) - B_{y1})/\sqrt{\mu_0 m_i N(z)}. \qquad (9)$$

Note that a different initialization using Hall magnetohydrodynamics (MHD) has also been used by *Krauss-Varban* [1993], and the results are quite similar to that from the above method. The parameter ranges used in our simulations are $30° \leq \theta_{nB} \leq 75°$, $0.01 \leq \beta_1 < 4$, and $-1080° < \Delta\Phi < 1080°$. The simulations are carried out for RDs with an initial transition width D ranging from $0.5L_i$ to $90L_i$, where L_i is the upstream ion inertial length. In the simulation the length per cell is $0.316L_i$. The system length used in this study is 1500 cells, or $475L_i$. Two buffer zones are set up at the two ends of the simulation domain with fixed magnetic field and plasma density. The ion number density $N_1 = N_2 = 100$ per cell.

In this paper, time is expressed in units of $t_0 \equiv \Omega_1^{-1}$, where $\Omega_1 = eB_1/m_i c$ is the upstream ion cyclotron frequency, e is the elementary charge, and c is the speed of light. The ion number density is normalized to $N_0 \equiv N_1$. The velocity is expressed in units of $V_0 \equiv V_{A1}$, where V_{A1} is the upstream Alfvén speed. The spatial coordinate is expressed in L_i, the magnetic field is expressed in B_1, the pressure is expressed in the upstream magnetic pressure $P_0 \equiv B_1^2/(2\mu_0)$, and the temperature is expressed in units of $T_0 = P_0/m_i N_0$.

3. Evolution of RDs and AWTs With Various Initial Widths and Field Rotation Angles

In this section we show the evolution of RDs and AWTs with a shock normal angle $\theta_{Bn} \equiv \tan^{-1}(B_{y1}/B_{x1}) = 75°$ and an upstream $\beta_1 = 1$. Cases with various initial transition width D are investigated. Other cases with different θ_{Bn} and β_1 are shown in section 4.

In case 1 an RD with initial field rotational angle $\Delta\Phi = 240°$ is simulated. The half width of the initial RD is chosen to be $D = 1.3L_i$. The initial profiles at $t = 0$ and the simulation results at $t = 80$ and 200 are shown in the first to the third columns of Figure 1. Presented in Figure 1 are, from the top, hodograms of the
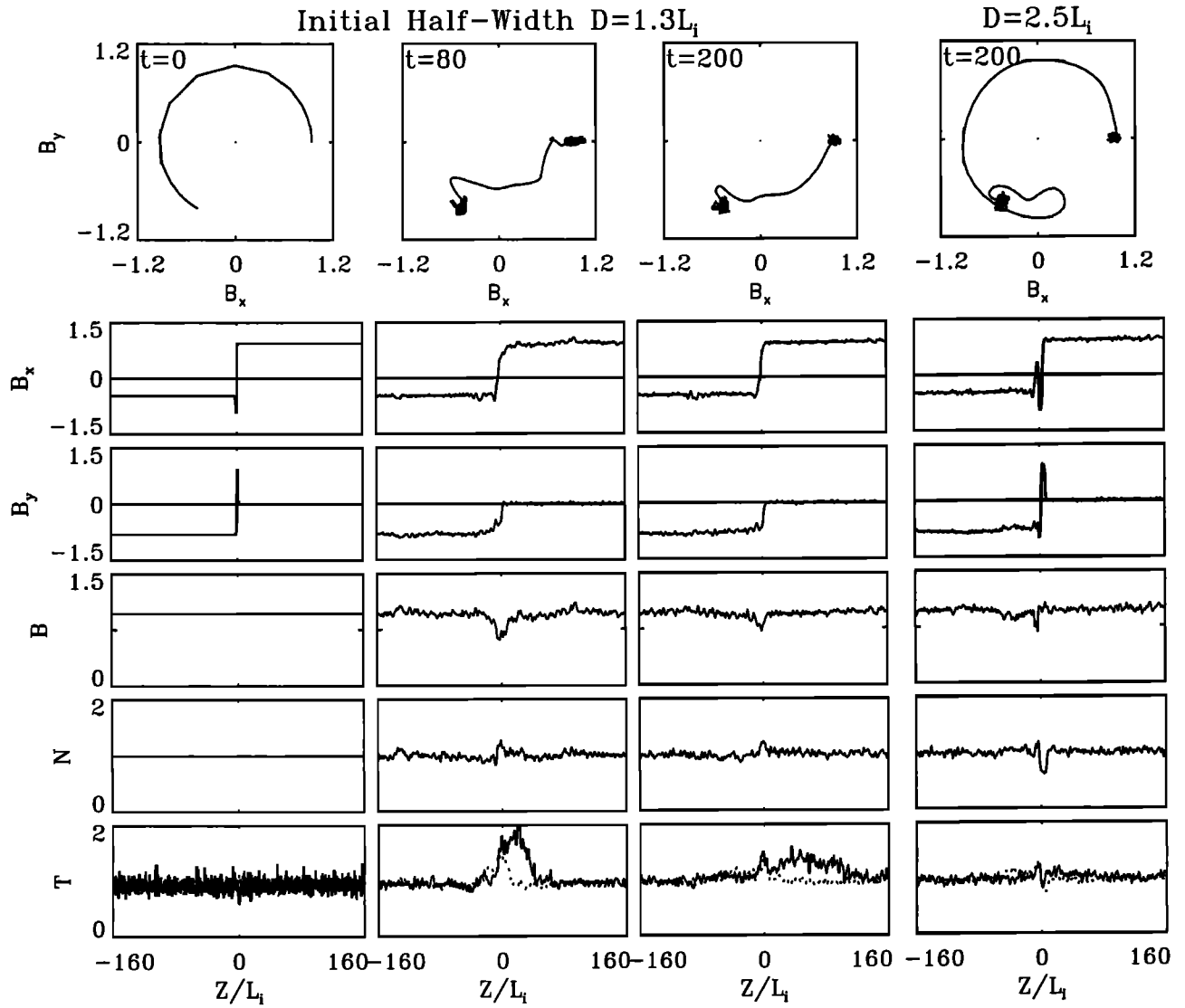
Figure 1. Hodograms of tangential magnetic field and spatial profiles of the normalized quantities B_x, B_y, magnetic field magnitude B, ion number density N, and ion temperatures T parallel (solid lines) and perpendicular (dotted lines) to the magnetic field obtained from case 1 at $t = 0$ (first column), $t = 80$ (second), and $t = 200$ (third) and from case 2 at $t = 200$ (fourth column). The upstream and downstream regions of the rotational discontinuity (RD) are on the $z > 0$ and $z < 0$ sides, respectively. Only the central part of the simulation domain is shown. In both cases, $\theta_{Bn} = 75°$, $\beta_1 = 1$, and the initial field rotation angle is in electron sense with $\Delta\Phi = 240°$. The initial width $D = 1.3L_i$ in case 1, while in case 2 the initial RD is wider with $D = 2.5L_i$.

tangential magnetic field and spatial profiles of the normalized quantities B_x, B_y, magnetic field magnitude B, ion number density N, parallel temperature $T_\parallel$ (solid lines), and perpendicular ion temperature $T_\perp$ (dotted lines). At $t = 80$ the magnetic field has changed from the initial right-handed rotation through the RD to a left-handed rotation of $\Delta\Phi = -120°$, as seen from the field hodogram. The RD has evolved to the new structure in which the change of the magnetic field takes a short path from upstream to downstream by reversing its sense of the rotation. In the new RD the magnetic field B decreases, and the density N increases. Two whistler waves have been generated and propagated from the RD into the upstream (right) and down-

stream regions, respectively. In the whistler waves, B and N increase in phase. The MHD fast mode speed is about $5.2C_I$ in the plasma with $\theta_{Bn} = 75°$ and $\beta = 1$. Since the upstream normal inflow speed is $\sim C_I$, the fast wave propagates with a speed of $\sim 4.2C_I$ in upstream against the inflow. In the downstream region the fast wave propagates with $\sim 6.2C_I$ along the flow direction. At $t = 80$ the fast wave has propagated a distance of $\sim 84L_i$ in the upstream region. The downstream whistler wave has reached a distance of $124L_i$. The parallel temperature $T_\parallel$ increases in the transition layer and in the region just upstream of the RD, and so does the density N. The perpendicular temperature $T_\perp$ increases in the transition region of the RD.

The changing of the internal structure of the RD can be understood as follows. The RD with $\Delta\Phi > 180°$ tends to evolve to a new structure in which the field rotation takes a shorter $\Delta\Phi$, while the net magnetic flux $I_y = \int B_y$ through the RD does not change. This is done by losing a 360° rotation of the field from the upstream edge, and thus in case 1 the new RD has a new $\Delta\Phi = \Delta\Phi|_{t=0} - 360° = -120°$, which corresponds to a left-handed or ion sense field rotation. In general, for a given $\Delta\Phi$ this reformation process depends on the initial wavelength D, which is related to the spatial gradient of the magnetic field components. If the RD is too narrow, as in case 1, a significant amount of ions that come into the RD from upstream cannot follow the rotation of the magnetic field. The electric current generated at the RD quickly changes the wave pattern of magnetic field, which may further enhance the difference between ion trajectories and the field line pattern because of the lower field and/or higher temperature in the transition region, until the new, short-pathed structure of magnetic field rotation is formed. We have traced ion trajectories in case 1 and found that by $t = 80$ about 50% of the incoming ions have been trapped in the RD and scattered, some returned to the upstream. The ion scattering leads to the increase in $T_\perp$ and N in the RD, and $T_\parallel$ increases in the upstream as the returned ions are accumulated. The flow energy is found to be reduced correspondingly. The enhancement in the thermal pressure in the RD transition causes a depression in B.

At $t = 200$, $T_\perp$ in the transition region of the new RD has gradually leveled down, although a peak in the pressure still exists. The magnetic field in the RD has developed into a more circular structure. The increase in $T_\parallel$ has spread over a wider region in the upstream. The central field transition region of the new RD is seen to be wider than that of the initial RD. The structure of the RD is found to be nearly the same as the simulation run further continues.

On the other hand, a larger initial width D results in a very different structure of RD. The fourth column of Figure 1 shows the results of case 2 at $t = 200$, in which the initial RD is the same as that in case 1, except a larger $D = 2.5L_i$ is assumed. At $t = 200$ the RD still holds the electron sense rotation. The magnetic field and the ion number density show an in-phase decrease in the electron sense RD. An additional fluctuation in B_x appears on the downstream side of the RD. At later times it is seen that the magnetic field rotates by 360° plus a reverse −120°. It then evolves to a new RD with $\Delta\Phi = -120°$ at $t \sim 500$, 6 times later than the turning time in case 1, in which D is reduced by 1/2. This result is similar to that obtained by *Krauss-Varban* [1993] for a an electron sense RD with a 270° field rotation. In the cases with small θ_{Bn}, which will be shown later in this section, some clear solitary waves are present as the RD evolves, and the waves propagate away from the RD as a new RD with a short-pathed field rotation forms.

In case 1 with a smaller D, the solitary wave-like structure at the downstream edge also appears in early times, but it is quickly destroyed in the RD transition. The wave amplitude becomes very small, and the wave propagates very slowly toward the upstream before it is destroyed. In general, a larger tangential magnetic field results in a larger scattering of ion particles that may destroy large-amplitude wave trains [e.g., *Lin and Lee*, 1991].

Figure 2 shows ion velocity distribution contours of the ions in case 1 (Figure 2a) and case 2 (Figure 2b) at $t = 80$ and at three different positions: in the upstream region around $z = 15.5L_i$, near the transition region around $z = 4.4L_i$, and in the transition region at $z = -1.9L_i$. Particles from nine grids around the above three z positions are used to produce the contours. The straight line in each plot is along the local magnetic field direction. In case 1 some backstreaming ions are seen in the V_x-V_z plot in upstream at $z = 15.5L_i$, with $V_x > 0$ and V_z near or greater than zero. The major population of the incident ions is seen to have a central flow velocity of $V_z < 0$ and $V_x < 0$. The parallel temperature $T_\parallel$ increases because of the field-aligned separation of the velocities of incident and returned ions. At $z = 4.4L_i$ the core of the backstreaming ions is seen clearly in the V_y-V_z plot, whose center is at $V_z \sim 0$. The number of ions also increases at this position. At $z = -1.9L_i$ the distribution plots show that both $T_\perp$ and $T_\parallel$ increase greatly because of the scattering of the ions.

In case 2, however, the ion velocity distributions at the three corresponding positions appear very different from those just shown for case 1. As shown in Figure 2b, no significant populations of backstreaming ions are present at $z = 15.5L_i$ and $z = 4.4L_i$. The plots at $z = -1.9$ in the RD transition do not show significant heating and ion scattering. Such distributions are quite common in the cases in which RD preserves its initial value of $|\Delta\Phi| > 180°$. The enhancement of ion transmission rate in RDs with a larger width D has also been shown by *Swift and Lee* [1983], although the results in their Figures 9 and 8 are only for thin RDs with a width up to one ion gyroradius.

Clearly, at a larger initial width D the RD can preserve its field rotation of $\Delta\Phi > 180°$ for a longer time, as seen from case 1 and case 2. This is because it takes time for the currents associated with the ion orbits to build up in the wide RD or for the solitary waves to form and propagate away from the RD in the cases with small θ_{Bn}.

We now show the evolution of RDs with ion sense field rotations. In cases 3 and 4, the initial RDs have an ion sense rotation of $\Delta\Phi = -240°$. In case 3 the initial transition width $D = 1.9L_i$, while in case 4 the initial RD is slightly wider with $D = 2.5L_i$. The results of case 3 at $t = 0$, 80, and 200 are shown in the first to third columns of Figure 3, and the results of case 4 at $t = 200$ are shown in the fourth column.

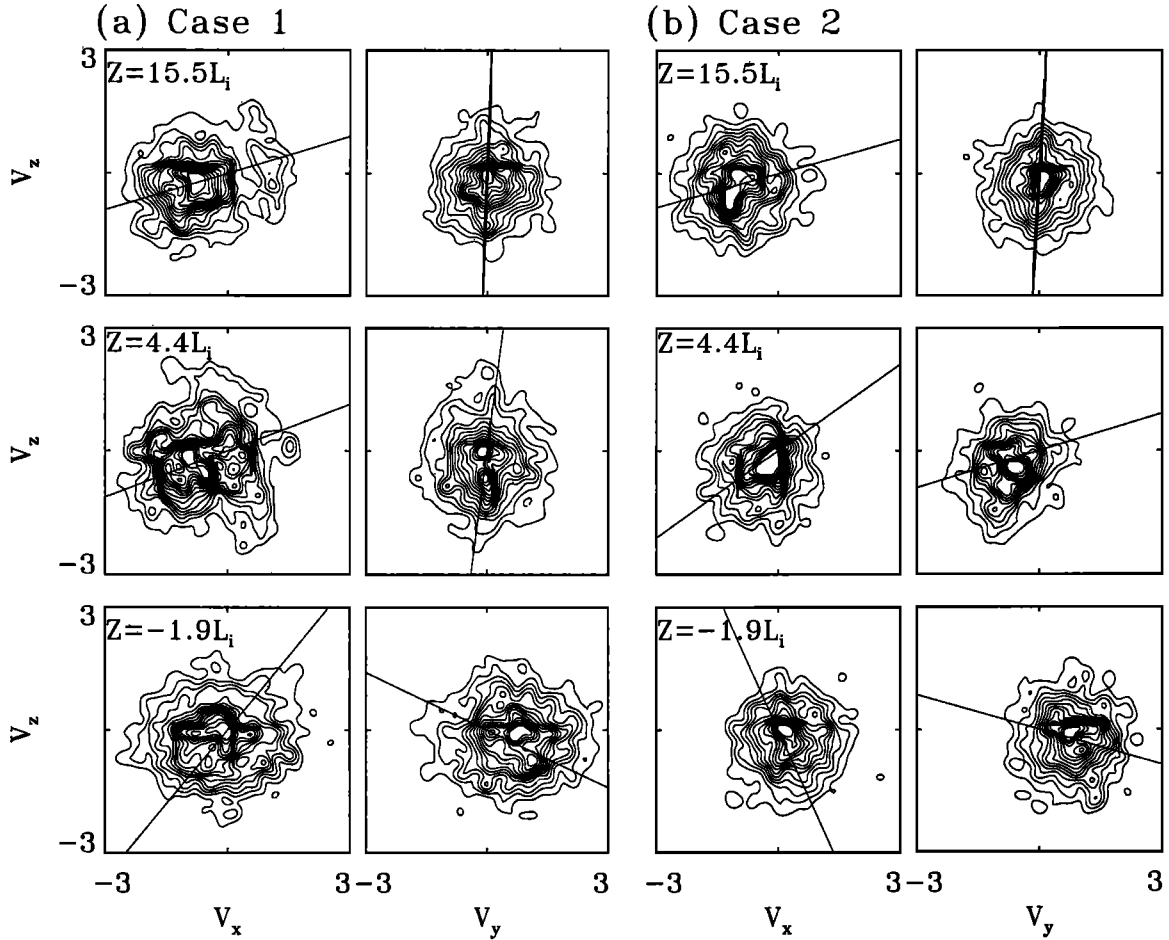In case 3, the magnetic field strength B becomes quite

Figure 2. Ion velocity distribution contours obtained from (a) case 1 and (b) case 2 at $t = 80$ and at $z = 15.5L_i$ in the upstream, $z = 4.4L_i$ near the RD transition, and $z = -1.9L_i$ in the transition region. The straight line in each plot is along the local magnetic field.

small at $t = 80$, while the ion sense field rotation still holds. Similar to case 1, two fast waves have propagated into the upstream and downstream regions as the RD evolves from $t = 0$, but they are two rarefaction waves in which N and B decrease and flow speed increases. In the transition region of the RD, the ion density N greatly increases. Such an antiphase relation between B and N is typical in the ion sense RDs [e.g., *Krauss-Varban*, 1993; *Lin and Lee*, 1993]. A long "foot" region has developed upstream of the RD, in which $T_{\parallel}$ increases and the flow (not shown) slows down, similar to case 1 when the field rotation is changing to the short path. At $t = 200$ the RD has developed into an electron sense structure, in which the magnetic field rotation takes a short path of $\Delta\Phi = 120°$. The thickness of the RD at $t = 200$ is much larger than at $t = 0$. An intermediate mode wave has developed at the downstream edge of the RD, in which the magnetic field decreases and the density and $T_{\perp}$ increases. This left-handed or ion sense dispersive wave propagates against the plasma with a speed smaller than the intermediate speed. This wave is gradually separated from the RD. In addition, a fast mode compressional wave, in which B and N increase,

is also seen propagating to the upstream while the RD reverses its sense of the field rotation. Similar to case 1, strong scattering of ions is found in the RD. On the other hand, in case 4 with a larger initial width D the field rotation is still left-handed by $t = 200$, although not quite circular, as seen from the field hodogram in the fourth column of Figure 3.

In the case with $\theta_{Bn} = 75°$, $\beta_1 = 1$, and $\Delta\Phi = -240°$, the "critical" initial half width that results in the reversal of the field rotation at $t = 200$ is found to be about $2.2L_i$, which is nearly the same as in the case with $\Delta\Phi = 240°$. In fact, for the cases with $\theta_{Bn} = 75°$ the critical width for various $|\Delta\Phi|$ is found to be nearly the same for $\Delta\Phi > 180°$ as for $\Delta\Phi < -180°$.

We now show in cases 5 to 7 the evolution of magnetic field rotations in Alfvén wave trains with an initial $\Delta\Phi = 720°$. The initial transition width $D = 11.1L_i$ in case 5, $D = 6.3L_i$ in case 6, and $D = 3.2L_i$ in case 7. The left two columns of Figure 4 show field hodograms and profiles of B_x and B_y in the AWT in case 5 at $t = 0$ and $t = 200$. It is seen that at $t = 200$ the AWT still contains two full rotations in the magnetic field. The field strength B is nearly a constant in the wave train.
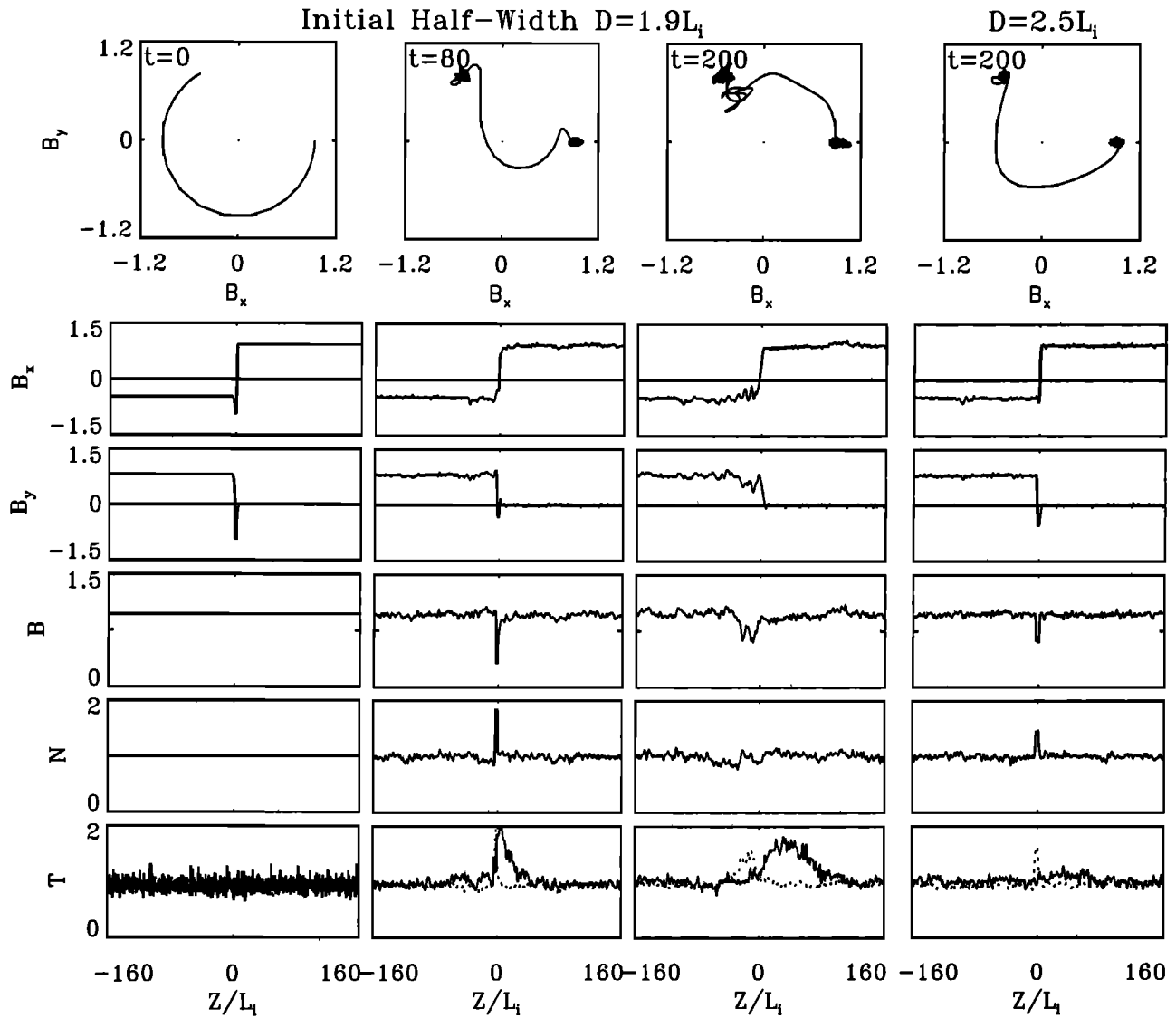
Figure 3. Same as Figure 1, except for case 3 $(D = 1.9L_i)$ and case 4 $(D = 2.5L_i)$ with ion sense field rotations $\Delta\Phi = -240°$.

The initial structure of the transition region remains almost unchanged as time passes.

For comparison, let us examine the results at $t = 200$ for cases 6 and 7. If D is not large enough, the RD or AWT may soon lose its first $n \times 360°$ field rotations when viewing from upstream, where n is an integer. For Alfvén wave trains with many field rotations, if D is very small, the tangential magnetic field may quickly reach its shortest path of $|\Delta\Phi| < 180°$. The third column of Figure 4 shows case 6 at $t = 200$. In this case with a narrower initial width D, the Alfvén wave train has lost a full $360°$ rotation before $t = 200$. At $t > 200$ the single rotation of $\Delta\Phi = 360°$ in the new AWT remains for a very long time because the width of the new AWT is quite large for $\Delta\Phi = 360°$. The minimum value of D at which the initial $\Delta\Phi = 720°$ can remain till $t = 200$ is $\sim 9.2L_i$. The fourth column of Figure 4 shows the results of case 7 at $t = 200$. In this case with

an even smaller initial width D, the magnetic field has lost its two full rotations with $\Delta\Phi = 720°$.

Next, we show two AWTs with $\Delta\Phi = 450°$, which contains a $360°$ plus a $90°$ rotation. These cases are different from cases 1 and 2 in the sense that after the AWT loses a $360°$ field rotation the final structure is an RD that is still right-handed. In case 8 the initial transition width $D = 5.1L_i$, while in case 9 a wider AWT with $D = 5.7L_i$ is assumed. The left and right columns of Figure 5 show the magnetic field and the ion density in Alfvén wave trains in case 8 and case 9 at $t = 200$, respectively. In case 8 the AWT has lost a $360°$ rotation and has become an RD with an electron sense field rotation of $\Delta\Phi = 90°$. In this case, field rotation does not extend beyond $450°$ before the $360°$ rotation is lost from the upstream edge, which is different from case 1 and 2 with initial $\Delta\Phi < 360°$. A small-amplitude wave appears at the upstream edge of
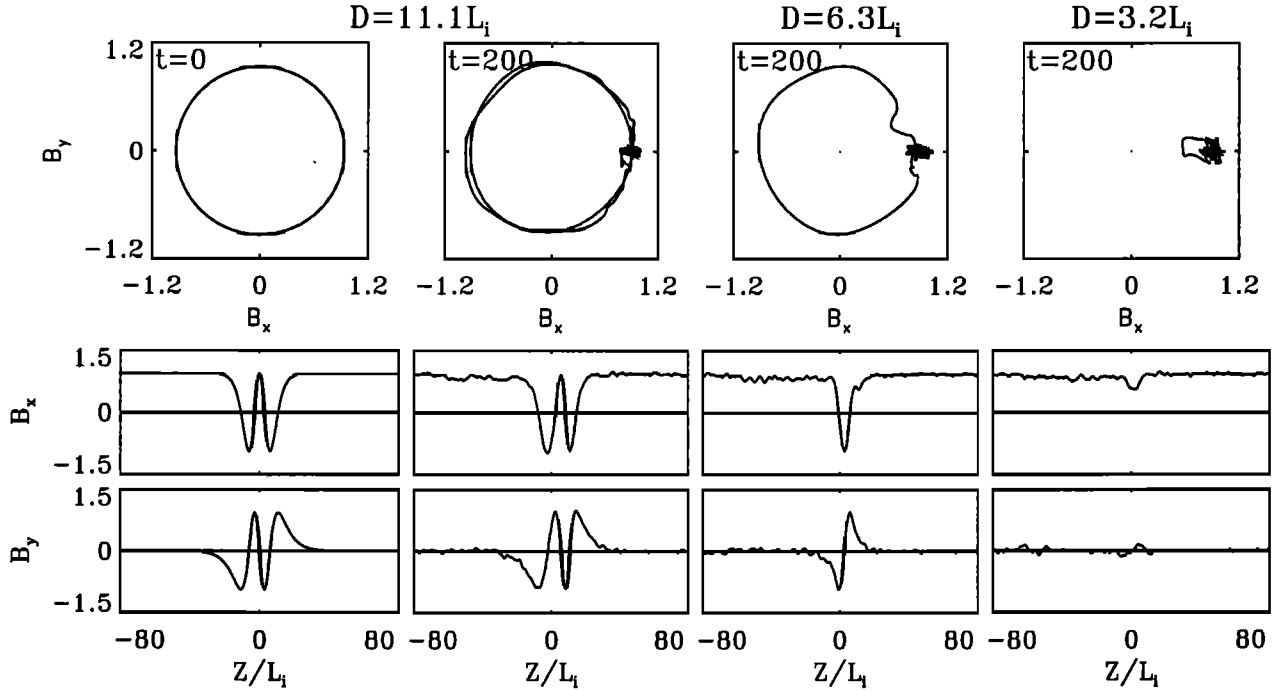
Figure 4. Evolution of magnetic field in three cases with initial $\Delta\Phi = 720°$, $\theta_{Bn} = 75°$, and $\beta_1 = 1$. The wide Alfvén wave train (AWT) in case 5 (left two columns) preserves the two field rotations, the narrower AWT in case 6 (third column) has lost one rotation, while very thin AWT in case 7 (right column) has lost all the field rotations.
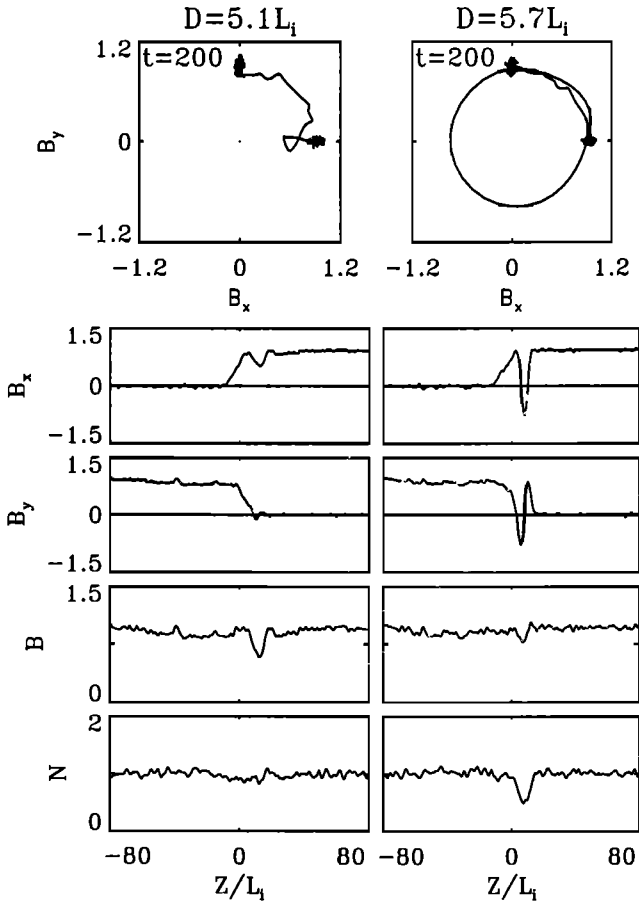

Figure 5. Structure of AWTs in case 8 (left column) and case 9 (right) with $\Delta\Phi = 450°$, $\theta_{Bn} = 75°$, and $\beta_1 = 1$.

the RD, in which B decreases. Later in the simulation, it is seen that in this small wave N also decreases. This wave may be an intermediate/ion cyclotron wave (also called an Alfvén/ion cyclotron wave). The wave speed is only slightly greater than the intermediate wave speed because of the large θ_{Bn}. Thus it propagates very slowly to upstream. On the other hand, in case 9 the magnetic field retains its large field rotation with $\Delta\Phi = 450°$ at $t = 200$, as seen in the right column of Figure 5.

4. Parameter Search and Applications

4.1. Dependence on $\Delta\Phi$

We have shown that by a certain final time, for example $t = 200$, a narrow RD or AWT may lose a multiple of 360° field rotations. It is found that the loss of the field rotations may occur later for wider RDs or AWTs. In order to see the evolution of magnetic field rotation in RDs and AWTs with various thickness D, we show in Figure 6a the critical time t_c (in units of Ω_I^{-1}), at which the magnetic field loses its first 360° rotation, as a function of D (in units of ion inertial length L_i) for cases with initial $\Delta\Phi = 240°$, 360°, 450°, and 720°. The shock normal angle is assumed to be $\theta_{Bn} = 75°$, and $\beta_1 = 1$. The change of magnetic field structure to that of a new rotation of ($\Delta\Phi - 360°$) is nonlinear in time. The RD or AWT may stay quite stable for a certain time before enough electric currents associated with the ion orbits build up and the amplitude of the 360° rotation starts to decay. During the decay of the field the starting and the end points of the first
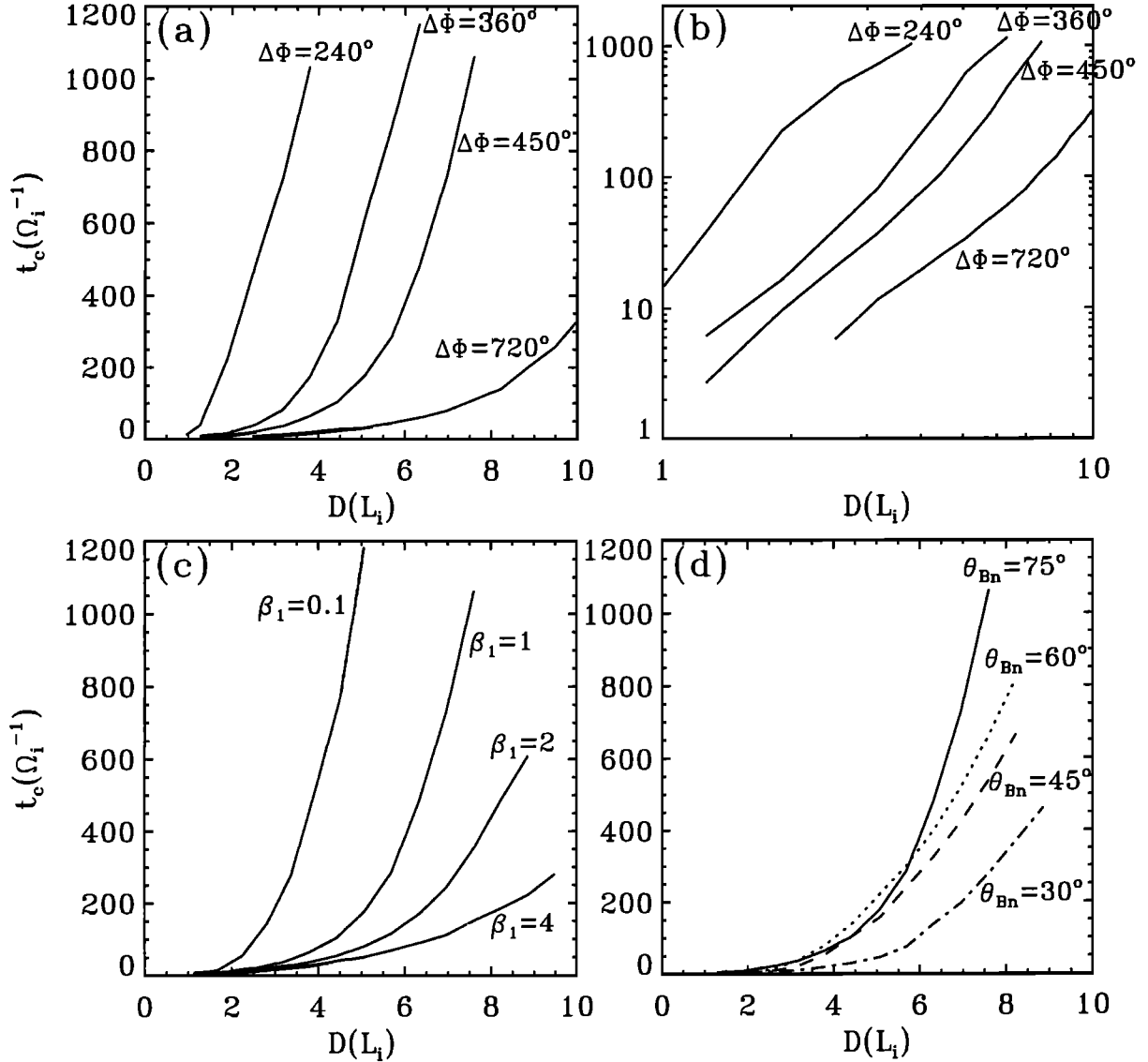
Figure 6. Figures 6a and 6b (6b in logarithm scales) show the critical time t_c as a function of initial width D for various initial field rotation angles $\Delta\Phi$, with $\theta_{Bn} = 75°$ and $\beta = 1$. Figure 6c shows the results for various β_1, with $\theta_{Bn} = 75°$ and $\Delta\Phi = 450°$. Figure 6d shows the results for various θ_{Bn}, with $\Delta\Phi = 450°$ and $\beta_1 = 1$. At t_c the RDs or AWTs lose just a 360° field rotation.

360° field rotation are nearly the upstream value with $B_{x1} > 0$ and $B_{y1} = 0$. We define the time t_c as the moment when the first 360° field rotation becomes small enough that it does not pass the origin $(B_x, B_y) = (0, 0)$ in the magnetic field hodogram.

In the case with $\Delta\Phi = 190°$ (not shown), $t_c \simeq 900$ for $D = L_i$, and it increases very rapidly with D. As $\Delta\Phi \to 180°$, t_c becomes infinity, consistent with the existence of stable RDs with $\Delta\Phi \leq 180°$. The increase of t_c is slower for a larger $\Delta\Phi$. Figure 6b shows t_c as a function of D in the logarithm scales. Approximate straight lines are seen for cases with various $\Delta\Phi$. Our simulations for cases with various initial conditions indicate that t_c varies with D nearly as

$$t_c = F(\Delta\Phi, \beta_1, \theta_{Bn}) D^{3.3 \pm 0.8}, \qquad (10)$$

where F is a function of $\Delta\Phi$, β_1, and θ_{Bn}. A similar

scaling of $t_c \sim D^{3.5}$ has also been obtained by *Krauss-Varban* [1993] for the case with $\Delta\Phi = 270°$, $\theta_{Bn} = 60°$, and ion $\beta_1 = 0.5$. For $\Delta\Phi > 540°$ one can also find the times for AWTs to lose two full field rotations, which are longer than those shown in Figure 6.

4.2. Application to the Magnetopause

Rotational discontinuities and Alfvén waves may be generated in magnetic reconnections at the dayside magnetopause. They may be convected from the X line near the subsolar region to the cusp with a typical convection speed of twice the Alfvén speed in the magnetosheath. For a magnetic field of 30 nT on the magnetosheath (upstream) side and an ion density of 10 cm^{-3}, the Alfvén speed is about 200 km/s. The convection speed is thus ~ 400 km/s. The characteristic convection time from the subsolar region to the cusp region magnetopause is
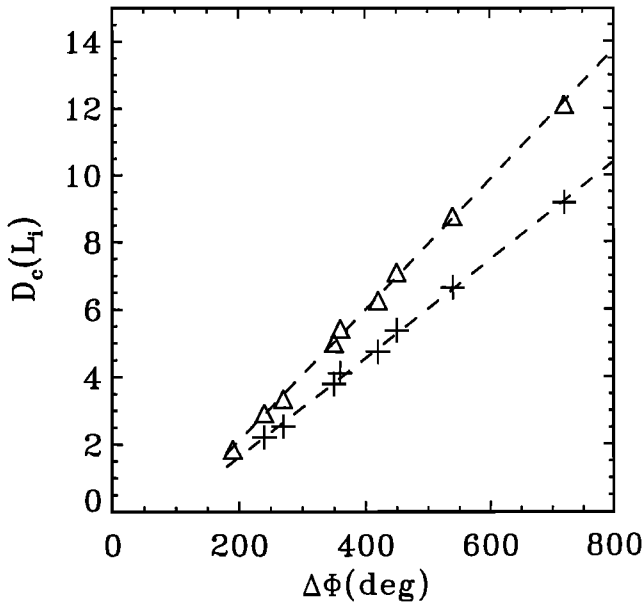
Figure 7. Minimum initial width D_c as a function of $\Delta\Phi$ for RDs or AWTs to preserve their initial $\Delta\Phi >$ 180° till $\Omega_1 t = 200$ (cross signs) and $\Omega_1 t = 500$ (open triangles). The latter time is nearly the typical transient convection at the dayside magnetopause. The calculation is conducted for $\theta_{Bn} = 75°$ and $\beta_1 = 1$.

about 3 min, corresponding to $t \sim 500\Omega_1^{-1}$. Consider an RD or Alfvén wave at a satellite position on the magnetopause that corresponds to $t = 200\Omega_1^{-1}$. Let D_c be a critical, or minimum, initial half width at which the RD loses just its first 360° field rotation at $t = 200$. The cross signs in Figure 7 show this critical width D_c as a function of the initial rotation angle $\Delta\Phi$. The results are obtained for $\theta_{Bn} = 75°$ and $\beta_1 = 1$ at the magnetopause. For RDs with an initial half width $D > D_c$, the magnetic field rotation of $|\Delta\Phi| > 180°$ remains for a time $t > 200\Omega_1^{-1}$. Also plotted in Figure 7 are similar minimum widths required for $t = 500\Omega_1^{-1}$, as shown by the open triangles.

The search has been conducted for $\Delta\Phi = 190°, 240°, 270°, 350°, 360°, 420°, 450°, 540°,$ and $720°$. The width D_c is seen to increase almost linearly with $\Delta\Phi$. This result indicates that a constant width is required for each unit angle of the field rotation. As discussed earlier, the minimum wavelength required by an RD should increase with $\Delta\Phi$, because $d\Phi/dz$ determines the gradient of the magnetic field components and thus the finite ion inertial effects that may produce random ion orbits or dispersive waves. We have also searched for D_c under negative rotation angles $\Delta\Phi = -190°$ to $-720°$. As mentioned earlier, it is found that in the cases with $\theta_{Bn} = 75°$ the critical widths D_c are almost the same as those for the corresponding positive angles $\Delta\Phi$.

Magnetic field rotation at the dayside magnetopause has been an interesting subject for decades. In the observation by *Sonnerup and Cahill* [1968] the magnetic field rotation across the magnetopause follows an

electron sense in both the Northern and the Southern Hemisphere. On the other hand, the observation by *Berchem and Russell* [1982] shows that the magnetic field rotates from the magnetosheath direction to the magnetospheric direction following the shortest angular path in either hemisphere. A recent study of tangential discontinuities at the dayside magnetopause by *Keyser and Roth* [1998] indicates that the sense of the field rotation may be very different under different magnetosheath flow conditions and thus the equilibrium conditions of the discontinuity. Our simulation suggests that the sense of magnetic field rotations at the magnetopause may depend on the thickness of the magnetopause current layer, which may in turn determine the direction of field-aligned currents generated from the magnetopause to the cusp ionosphere.

4.3. Dependence on β_1

Next, we show case 10 with a low beta, $\beta_1 = 0.1$. This case is similar to case 8, with $\theta_{Bn} = 75°$ and $\Delta\Phi = 450°$. The initial width $D = 3.0L_i$. The left, middle, and right columns of Figure 8 show field hodograms and spatial profiles of various physical quantities in case 10 at $t = 0, 80,$ and 200, respectively. Similar to cases with $\beta_1 = 1$, two whistler waves have propagated into the upstream and downstream regions at $t = 80$. The temperature increases in the transition region of the AWT, and the magnetic field decreases. The initial AWT gradually evolves to a new rotational discontinuity with $\Delta\Phi = 450° - 360° = 90°$. As the AWT evolves, a strong enhancement in N and a decrease in B appear just downstream of the AWT. This structure propagates with nearly the slow mode speed against the flow. Both $T_\parallel$ and $T_\perp$ also increase. At $t = 200$ the new RD with the shorter field rotation has formed. The field rotation is still right-handed in the RD transition. The slow mode structure is continuously released from the AWT as it is turning into the new RD and is extending to a longer region in downstream. The wave amplitude is seen to be reduced at later times, perhaps partly owing to Landau damping and partly owing to the RD reaching a more stable structure. On the upstream side an intermediate mode solitary wave with a right-handed field rotation appears, as shown in the right column of Figure 8. In this wave, B and N decrease significantly, and T increases. This solitary wave has been separated from the RD and is seen very clearly in this case with the small β_1. Note that in the low beta limit the dispersive wave structures due to ion inertial effects approach the results from two-fluid models.

Figure 6c presents the t_c versus D curves in cases with various β_1. The critical time t_c for RDs or AWTs to lose the first 360° field rotation is found to decrease as β_1 increases from 0.1 to 4.0. Cases with various β_1 have also been simulated to search for the minimum initial widths D_c at which the initial $\Delta\Phi$ can remain till $t = 200$. The results are shown in Figure 9, which are obtained from $\theta_{Bn} = 75°$, $\Delta\Phi = 450°$, and $\beta_1 = 0.01$-
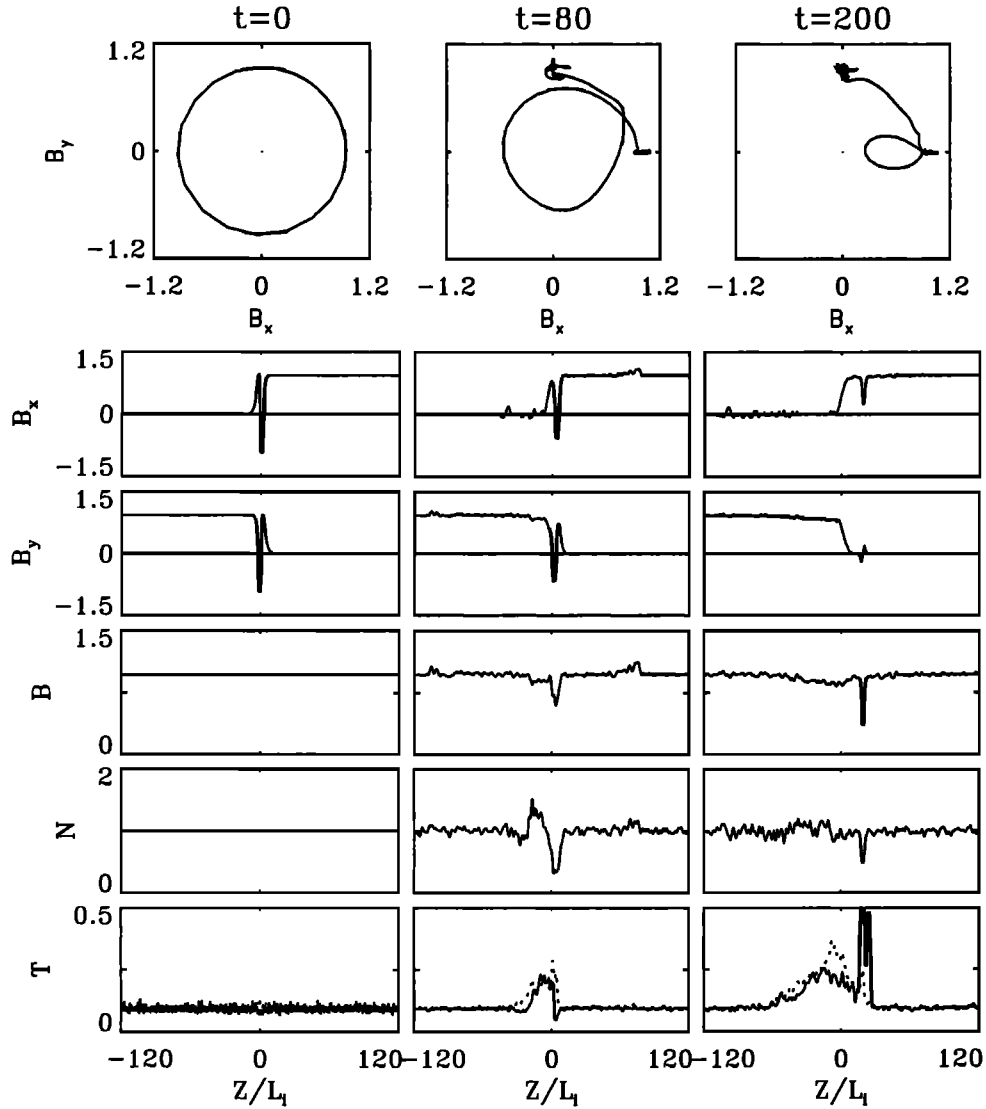
Figure 8. Field hodograms and spatial profiles of various quantities at $t = 0$, 80, and 200 in case 10 with $\beta_1 = 0.1$, $\Delta\Phi = 450°$, $\theta_{Bn} = 75°$, and $D = 3.0L_i$.

4.0. Note that much denser grids have been used in the simulation of cases with $\beta_1 \leq 0.2$ in order for the grid size to be smaller than ion gyroradii. It is seen that D_c is nearly proportional to $\sqrt{\beta_1}$ for $\beta_1 \geq 0.1$, or $\sqrt{\beta_1} > 0.3$. This is because the critical width is determined by ion trajectories in the RD and thus ion gyroradius, which is proportional to $\sqrt{\beta_1}$ at a given Alfvén speed and a given magnetic field. On the other hand, in the cold plasma with low $\beta_1 < 0.1$ the ion particle effects become less important, and intermediate mode solitary waves are seen to propagate out and cause the spreading of the initial AWT. The critical width D_c is nearly a constant. As ion $\beta_1 \rightarrow 0$, the width of RD or AWT is determined by the wavelengths of dispersive waves due to ion inertial effects. *Hau and Sonnerup* [1991] have studied the structure of RDs using a gyroviscous two-fluid model. They have also shown that including the Hall term alone in the generalized Ohm's law but excluding gyroviscous stresses leads to an RD of infinite thickness. Note that

two-fluid models are only approximately appropriate as ion β approaches zero. The structure of RDs with ion $\beta = 0$ has been shown by *Vasquez and Cargill* [1993] using hybrid simulations.

4.4. Dependence on θ_{Bn}

So far we have shown the results for $\theta_{Bn} = 75°$. In the following, cases with $\theta_{Bn} = 60°$, 45°, and 30° are presented. It is found that the evolution of RD or AWT in cases with $\theta_{Bn} = 60°$ is qualitatively similar to that in the cases with $\theta_{Bn} = 75°$, although the evolution of solitary waves released from RD or AWT is slightly different. The evolution of an AWT in case 11 is shown in Figure 10, in which $\theta_{Bn} = 60°$, $\beta_1 = 0.1$, $\Delta\Phi = 450°$, and $D = 4.4L_i$.

Figure 10 shows the magnetic field structure at $t = 0$, 120, 160, and 200. At $t = 120$ the leading part of AWT with the 360° field rotation still exists in the AWT, but it has started to be separated from the trailing
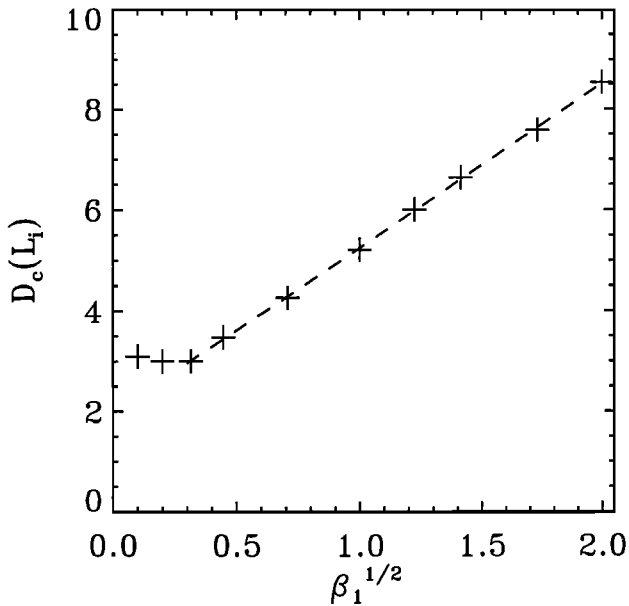
Figure 9. Cross signs show D_c as a function of $\beta_1^{1/2}$ for cases with $\theta_{Bn} = 75°$ and $\Delta\Phi = 450°$.

part with the 90° field rotation. At $t = 160$ a right-handed solitary wave appears in the upstream, which is evolved from the part of the AWT with the 360° field rotation. The initial AWT has evolved to a new RD with $\Delta\Phi = 90°$ after losing the 360° rotation. This right-handed intermediate/ion cyclotron solitary wave contains a decrease in B and N. This result is different from that in case 8, which also has $\Delta\Phi = 450°$ and $\beta_1 = 1$ but the shock normal angle $\theta_{Bn} = 75°$. In case 8 the 360° solitary wave is destroyed before it propagates out of the AWT. The upstream wave at $t = 160$ in case 11, however, disappears at $t = 200$, as seen from the right column of Figure 10.

As θ_{Bn} decreases, the process through which an RD or AWT evolves to a new RD or AWT with a smaller $|\Delta\Phi|$ becomes quite different in the parameter range of our simulations. The small ratio of the tangential to normal magnetic field in the less oblique cases weakens the scattering of ion orbits. Ions penetrate RD more easily along the magnetic field lines. The upstream and downstream solitary waves released from the RD or AWT are seen to last for a long time as they propagate away from the new RD. These waves are generated by the finite ion Larmor radius effects. For less oblique RDs the group velocity of wave packets of the normal modes associated with RDs can propagate out more easily along the field lines [*Goodrich and Cargill*, 1991; *Vasquez and Cargill*, 1993]. The RDs with $\theta_{Bn} < 45°$ are usually thicker than more obliquely propagating RDs.

In case 12, $\theta_{Bn} = 45°$, $\beta_1 = 1$, $\Delta\Phi = 450°$, and the the initial AWT is relatively narrow with $D = 4.1L_i$. Figure 11 shows hodograms of tangential magnetic field and spatial profiles of various quantities at $t = 0, 70,$ 130, and 210. At $t = 70$ the AWT is seen to be much

wider than at $t = 0$. A whistler wave is present in the upstream region, in which B and N peak at $z \simeq 61L_i$. The leading part of the AWT which contains a right-handed 360° field rotation has started to be separated from the trailing part. At $t = 130$ the initial AWT has spread into an intermediate mode solitary wave with nearly 360° field rotation and a new RD with $\Delta\Phi = 90°$. Both $T_\parallel$ and $T_\perp$ remain nearly constant throughout the simulation domain. The right-handed intermediate/ion cyclotron wave propagates upstream of the new RD with a speed larger than the inflow speed, in which the variations in B and N are in phase. At $t = 210$ this solitary wave has propagated to $z \simeq 40L_i$ and has become weaker. It is found to maintain its main structure for a long time, which is very different from cases with larger θ_{Bn}. The structure of the new RD with $\Delta\Phi = 90°$, in which B and N are nearly constant, is quite stable.

In the cases with θ_{Bn} around or smaller than 45°, the critical width D_c may be very different for RDs or AWTs which initially have the same $|\Delta\Phi|$ but different field rotation senses. This feature is quite different from the cases with large angles of θ_{Bn}. As shown earlier, for $\theta_{Bn} = 75°$ the critical number D_c is almost the same for the same $|\Delta\Phi|$. For $\theta_{Bn} > 45°$, nonlinear scattering of ions due to rapid changing of magnetic field direction plays an important role in the process in which the $\pm360°$ field rotation is lost. The generation of the random currents due to ion orbits is mainly determined by the ratio between ρ_i and D_i, where ρ_i is the ion gyroradius and D_i is the width of RD per unit degree of field rotation. The field rotation sense of the initial RD does not play a significant role. The $\pm360°$ field rotation is carried away mainly by fast or intermediate waves generated at the RD. These waves are very different in RDs with different senses of field rotations.

In case 13 we show the evolution of an AWT which is similar to that in case 12, except with an ion sense field rotation of $\Delta\Phi = -450°$. Note that in these cases with small θ_{Bn}, the minimum initial width D_c at which $\Delta\Phi$ can remain till a certain final time is smaller for electron sense RDs or AWTs than for ion sense RDs. In the case with $\theta_{Bn} = 75°$, $\beta_1 = 1$, and $\Delta\Phi = 450°$, $D_c \simeq 5.7L_i$, while for $\theta_{Bn} = -450°$ the minimum width $D_c \simeq 10L_i$. In case 13 we assume the initial width $D = 8.2L_i$, which is larger than that in case 12 but still smaller than the critical D_c.

Figure 12 shows various quantities at $t = 0, 60,$ and 110. Since the initial AWT carries an ion sense magnetic field variation, its first 360° field rotation is left-handed. The left-handed intermediate wave propagates with a speed that is smaller than the intermediate mode speed, and thus it cannot propagate into the upstream as in case 12. Instead, the AWT loses its $\Delta\Phi$ by releasing small-amplitude waves to both upstream and downstream. At $t = 60$, $T_\perp$ is seen to have increased by a factor of 2 in the AWT; the density N also increases greatly. The magnetic pressure decreases, and the variation of magnetic field through the AWT is not circular, as seen from the field hodogram. Again, some
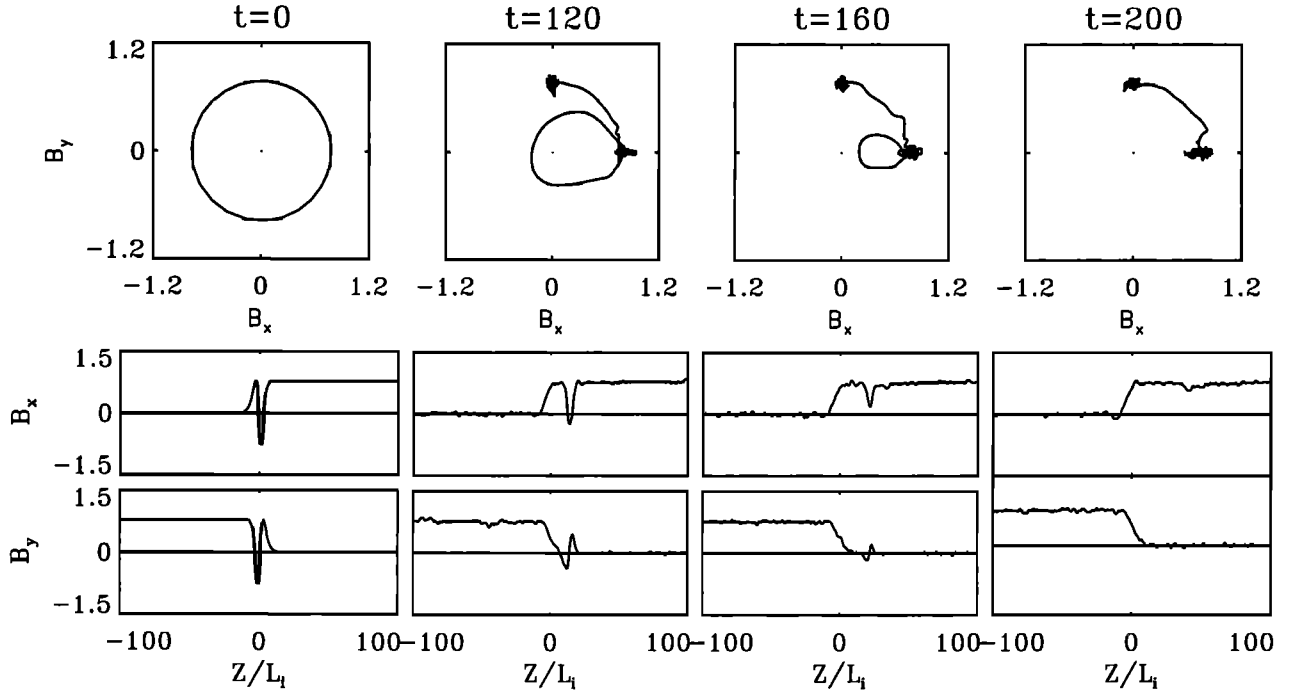
Figure 10. Results of case 11 with $\theta_{Bn} = 60°$, $\beta_1 = 1$, $\Delta\Phi = 450°$, and $D = 4.4L_i$.

whistler waves have propagated into the ambient plasmas. At $t = 110$ the initial unstable AWT has turned into a new RD with $\Delta\Phi = -90°$. A right-handed intermediate mode wave with a decrease in B and N is seen on the upstream side of the RD transition. This wave continuously propagates away in the upstream. A long downstream wave structure is also present, which propagates in the $-x$ direction. In the leading part of the downstream wave, B and N increase. The density structure of this wave is more complicated in the trailing part, indicating that the wave structure is changing as it is released from the AWT while the new RD is formed. The RD is quite stable, and its width is nearly a constant. We have also simulated cases with $\theta_{Bn} = 30°$, and the results are similar to the cases with $\theta_{Bn} = 45°$.

Figure 6d shows the critical time t_c as a function of the initial width D for $\theta_{Bn} = 75°$, $60°$, $45°$, and $30°$. The calculation is conducted for AWTs with $\beta_1 = 1$ and $\Delta\Phi = 450°$. Again, the relation between t_c and D satisfies equation (10). It is seen that as θ_{Bn} decreases from $75°$ to $30°$, the RDs or AWTs lose a $360°$ field rotation at a much shorter time. Nevertheless, at relatively short widths $D < 5.5L_i$, the time t_c for $\theta_{Bn} = 60°$ is slightly larger than that for $\theta_{Bn} = 75°$. This is because in the less oblique AWTs with $\theta_{Bn} = 60°$, the ion scattering in the rotational magnetic field is weaker and thus t_c is larger. As D increases, the disintegration of the less oblique AWTs may be dominated by the spreading of solitary waves, which is faster as θ_{Bn} becomes smaller.

4.5. Application to the Solar Wind

Parker [1991] suggested that Alfvén waves can heat solar coronal particles in the coronal holes. *Lee et al.* [1996] proposed that rotational discontinuities and

Alfvén waves may be generated as a result of magnetic reconnections in the coronal holes. Simulations by *Lin and Lee* [1993] and *Ma and Lee* [1999] indicated that rotational discontinuities may be imbedded in Alfvén waves in the outflow region of magnetic reconnection. Assume that the relations between t_c and D shown in Figure 6 are also valid for large D and t. We can estimate the minimum widths of Alfvén wave trains (i.e., $|\Delta\Phi| > 360°$) in the solar wind in order for them to exist and be observed near the Earth at $1AU$.

Observations have indicated that more RDs are found in high-speed streams (500-800 km/s at 1 AU) emanating from coronal holes [*Neugebauer*, 1992]. For a solar wind speed of 500 km/s it takes about 3.5 days for AWTs to travel a distance of $r \sim 1$ AU. The proton density decreases from the surface of the Sun as $\sim r^{-2}$. The radial component of the magnetic field varies as $\sim r^{-2}$, and the azimuthal magnetic field varies as $\sim r^{-1}$. As the AWTs propagate away from the Sun in the nonuniform solar wind, their shock normal angle may change. Observations indicate that RDs in the solar wind are usually evolving with time and that the range of θ_{Bn} is wide [e.g., *Neugebauer*, 1989]. For a rough estimate, let us use the plasma and magnetic field conditions at 0.5 AU as an average. Given that the observed proton density at 1 AU is ~ 5 cm^{-3}, the density at 0.5 AU is estimated to be 20 cm^{-3}, corresponding to $L_i \sim 51$ km. The magnetic field strength at 1 AU is ~ 6 nT. Assuming a Parker spiral angle of $45°$, the radial and the azimuthal components of the magnetic field at 1 AU are about $B_r \simeq B_\phi \simeq 4.24$ nT, which correspond to $B_r \simeq 17$ nT and $B_\phi \simeq 8.5$ nT at 0.5 AU. The total field at 0.5 AU is ~ 19 nT, and thus the ion gyro-frequency $\Omega_1 \sim 1.82$ s^{-1}. The propagation time of
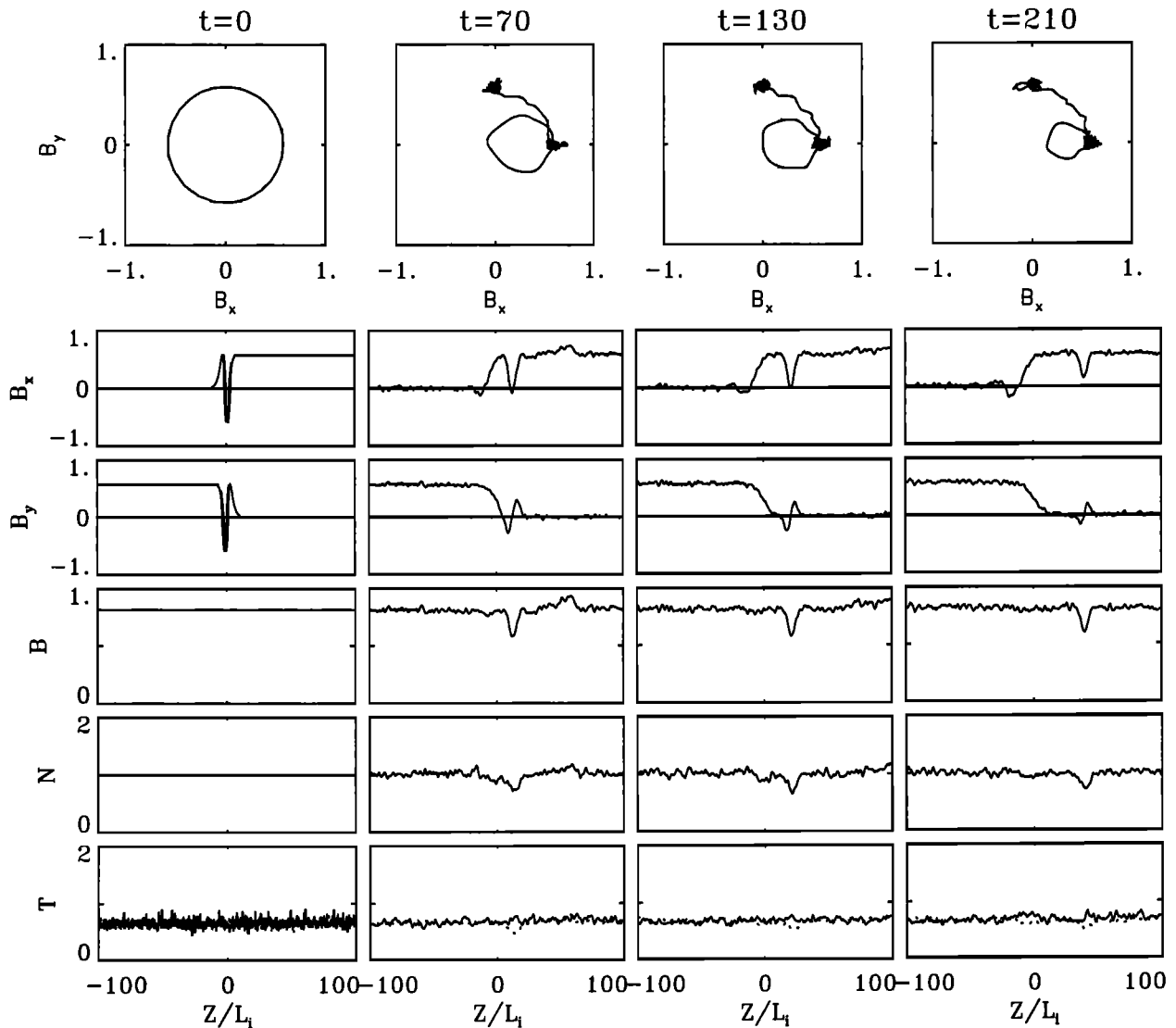
Figure 11. Evolution of the electron sense AWT in case 12 with $\theta_{Bn} = 45°$, $\beta_1 = 1$, $\Delta\Phi = 450°$, and $D = 4.1L_i$.

3.5 days then corresponds to $t \sim 5.5 \times 10^5\Omega_1^{-1}$. Assuming this is the minimum time required for the existence of AWTs, the width D corresponding to this time is the minimum width of AWTs. For cases with $\beta \sim$ unity the minimum half width of AWTs per 360° field rotation is estimated as $\simeq 60L_i \simeq 3060$ km for $\theta_{Bn} = 30°$, and it is nearly $44L_i \simeq 2250$ km for $\theta_{Bn} = 75°$. The minimum lengths of AWTs per 360° rotation are therefore estimated to be on the order of thousands of kilometers. In an observation by *Tsurutani and Gonzalez* [1987], long Alfvén wave trains with many large-amplitude fluctuations in magnetic field have been found in the solar wind, which has a wavelength of ~ 30 Earth radii.

To our knowledge, so far there has been no report of rotational discontinuities with $|\Delta\Phi| > 180°$ in the solar wind. This phenomenon may be understood as follows. It has been suggested that RDs may be generated by magnetic reconnections associated with microflares [*Lee et al.*, 1996]. Consider that the reconnection occurs in a thin current sheet. The rotational discontinuities gen-

erated from the X line may also be thin, with their widths not more than a few ion inertial lengths in the low-beta plasma. RDs with $|\Delta\Phi| > 180°$ would remain for hundreds to thousands of ion gyroperiods, as inferred from Figure 6. For $B \sim 10$ G in the coronal hole, this duration corresponds to a time of less than 0.1 s. Therefore the RDs would easily lose a 360° field rotation to become a new RD with $|\Delta\Phi| < 180°$ as they propagate out into the solar wind. On the other hand, RDs with $|\Delta\Phi| > 180°$ may be more easily found at the magnetopause, where the ion gyroperiod is long and the characteristic convection distance is short.

An alternative view has also been proposed for the formation of rotational discontinuities in the solar wind. *Cohen and Kulsrud* [1974] showed that in the ideal MHD approximation, nonlinear hydromagnetic fluctuations propagating along the mean magnetic field may steepen into shocks and subsequently evolve into purely Alfvénic fluctuations or rotational discontinuities. Numerical simulations were also carried out to show that
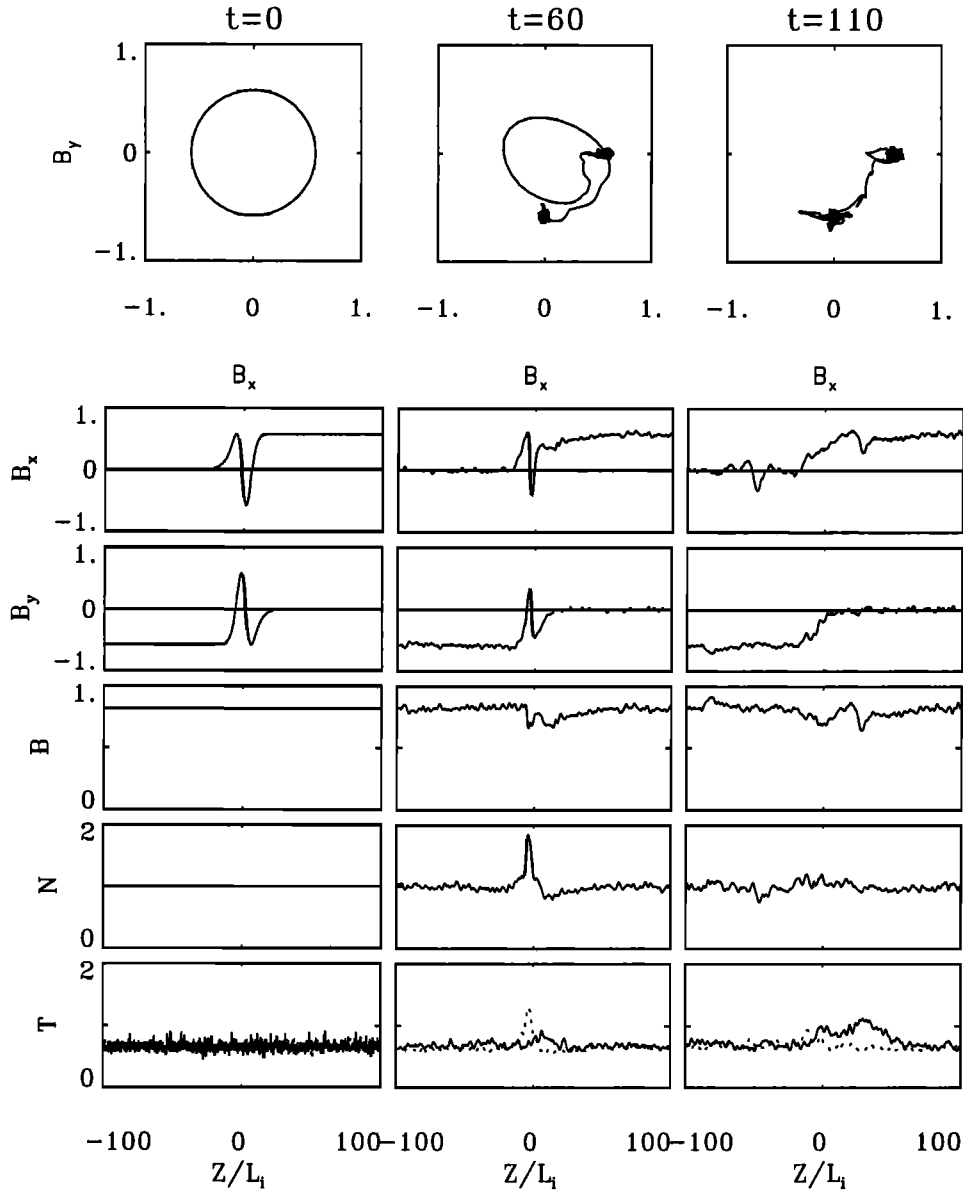
Figure 12. Evolution of the ion sense AWT in case 13 with $\theta_{Bn} = 45°$, $\beta_1 = 1$, $\Delta\Phi = -450°$, and $D = 8.2L_i$.

the Alfvénic fluctuations can steepen and generate imbedded RDs [*Vasquez and Hollweg*, 1996, 1998a, b; *Medvedev et al.*, 1997]. *Vasquez and Hollweg* [1998b] suggested that in order to account for the frequent occurrence of the RDs with small θ_{Bn}, Alfvénic fluctuations with imbedded RDs must be evolving through a succession of arc-polarized or spherically polarized waveforms. The hybrid simulation of *Vasquez and Hollweg* [1996] showed that RDs with $|\Delta\Phi| \leq 180°$ are always produced by steepening from linearly polarized Alfvén waves because of the geometrical constraints of the Alfvén waves *Barnes and Hollweg* [1974].

5. Summary

In summary, we have carried out 1-D hybrid simulations to study the structure of rotational discontinuities and large-amplitude Alfvén wave trains. In particular,

the investigation is conducted for the evolution of magnetic field rotations through RDs or AWTs which initially have a field rotation angle of $|\Delta\Phi| > 180°$. The simulation has been performed for RDs with a broad range of thickness D.

It is found that for a given initial half width D the RDs or AWTs with $|\Delta\Phi| > 180°$ lose $\pm360°$ rotation in magnetic field at a time t_c, and the magnetic field rotation takes a shorter path through the RD or AWT. At $t < t_c$, however, RDs and AWTs preserve the initial field rotation angle $\Delta\Phi$. The critical time t_c is estimated to be $t_c \simeq F(\Delta\Phi, \beta_1, \theta_{Bn})D^{3.3\pm0.8}$.

The evolution of magnetic field rotation through RDs and AWTs as a function of the initial $\Delta\Phi$, the upstream β_1, and the shock normal angle θ_{Bn} is studied by examining the structure of the magnetic field at a certain final time, which corresponds to a given transient convection time at the dayside magnetopause and in the

solar wind, for cases with various initial width D. It is found that there exists a critical initial width D_c such that for $D > D_c$, RDs and AWTs can preserve their initial rotation angle $|\Delta\Phi| > 180°$ for a time longer than a given transient convection time in space plasmas. For $D < D_c$, RDs or AWTs may quickly lose $n \times 360°$ field rotations, where n is an integer, until a smallest rotation angle $|\Delta\Phi| < 180°$ is reached. The losing of magnetic field rotations in RD or AWT starts from its upstream edge. For $\theta_{Bn} = 75°$, $\Delta\Phi = 190°$ to $720°$, and $\beta_1 = 0.01$ to 4, the minimum widths D_c are on the order of a few to tens of ion inertial lengths L_i. It is linearly proportional to the field rotation angle $|\Delta\Phi|$ across the initial RD or AWT, increases linearly with $\sqrt{\beta_1}$ for $\beta_1 \geq 0.1$, and decreases with θ_{Bn}. This is equivalent to t_c decreasing with increasing $\Delta\Phi$ and β_1 and decreasing θ_{Bn}. In the cases with low $\beta_1 < 0.1$, solitary waves are found to propagate away during the disintegration of RDs and AWTs, and the width D_c is nearly constant because the ion particle effects are relatively weak. For Alfvén wave trains ($|\Delta\Phi| > 360°$) in the solar wind to maintain more than one rotation of magnetic field during their convection time from solar corona to about 1 AU, their minimum widths per $360°$ rotation are found to be on the order of thousands of kilometers.

The mechanism by which an RD or AWT with $|\Delta\Phi| > 180°$ evolves to a new RD or AWT with a smaller $|\Delta\Phi|$ appears to be quite different for cases with $\theta_{Bn} \leq 45°$ and for highly oblique cases with $\theta_{Bn} > 45°$. For highly oblique cases, strong nonlinear scattering of ions due to the rapid change of magnetic field direction plays an important role in the reformation of RD and AWT. The generation of the electric currents due to ion orbits is mainly determined by the ratio between the ion gyroradius and the field rotation rate $d\Phi/dz$. The field rotation sense of the initial RD does not play a significant role.

On the other hand, in the cases with $\theta_{Bn} \leq 45°$, ions penetrate RD more easily along the magnetic field lines. The $\pm 360°$ field rotations are carried away mainly by fast or intermediate waves that are generated at RD owing to finite ion Larmor radius effects. These waves are very different in RDs with different senses of field rotations. In RD with an electron sense rotation, the right-handed 360° rotation in the magnetic field can be easily carried away from upstream through an intermediate/ion cyclotron wave. In an ion sense RD, however, $|\Delta\Phi|$ is carried away by many small-amplitude upstream and downstream waves. In cases with $\theta_{Bn} \leq 45°$, the values of D_c are quite different for RDs with the same magnitude of $\Delta\Phi$ but different rotation senses.

References

Alexander, C. J., M. Neugebauer, E. J. Smith, and S. J. Bame, The relation of solar wind structure to hydromagnetic discontinuities, *Tech. Note NCAR/TN-306+Proc*, Natl. Cent. for Atmos. Res., Boulder, Colo., p. 341, 1987.

Barnes, A., and J. V. Hollweg, Large-amplitude hydromagnetic waves, *J. Geophys. Res.*, *79*, 2302, 1974.

Berchem, J., and C. T. Russell, Magnetic field rotation through the magnetopause: ISEE 1 and 2 observations, *J. Geophys. Res.*, *87*, 8139, 1982.

Nature and origin of directional discontinuities in the solar wind, *J. Geophys. Res.*, *76*, 4360, 1971.

Buti, B., Stochastic and coherent processes in space plasmas, in *Cometary and Solar Plasma Physics*, p. 221, World Sci., River Edge, N. J., 1988.

Cohen, R. H., and R. M. Kulsrud, Nonlinear evolution of parallel-propagating hydromagnetic waves, *Phys. Fluids*, *17*, 2215, 1974.

Goodrich, C. C., and P. J. Cargill, An investigation of the structure of rotational discontinuities, *Geophys. Res. Lett.*, *18*, 65, 1991.

Hada, T., C. F. Kennel, and B. Buti, Stationary nonlinear Alfvén waves and solitons, *J. Geophys. Res.*, *94*, 65, 1989.

Hau, L.-N., and B. U. O. Sonnerup, Self-consistent gyroviscous fluid model of rotational discontinuities, *J. Geophys. Res.*, *96*, 15,767, 1991.

Kennel, C. F., B. Buti, and R. Pellat, Nonlinear, dispersive, elliptically polarized Alfvén waves, *Phys. Fluids*, *31*, 1949, 1988.

Keyser, J. D., and M. Roth, Magnetic field rotation at the dayside magnetopause: AMPTE/IRM observations, *J. Geophys. Res.*, *103*, 6663, 1998.

Krauss-Varban, D., Structure and length scales of rotational discontinuities, *J. Geophys. Res.*, *98*, 3907, 1993.

Landau, L. D., and E. M. Lifshitz, *Electrodynamics of Continuous Media*, Pergamon, New York, 1960.

Lee, L. C., and J. R. Kan, Structure of the magnetopause rotational discontinuity, *J. Geophys. Res.*, *87*, 139, 1982.

Lee, L. C., J. R. Kan, and S.-I. Akasofu, On the origin of the cusp field-aligned currents, *J. Geophys.*, *57*, 217, 1985.

Lee, L. C., L. Huang, and J. K. Chao, On the stability of rotational discontinuities and intermediate shocks, *J. Geophys. Res.*, *94*, 8813, 1989.

Lee, L. C., Y. Lin, and G. S. Choe, Generation of rotational discontinuities by magnetic reconnection associated with microflares, *Sol. Phys.*, *163*, 335, 1996.

Lepping, R. P., and K. W. Behannon, Magnetic field directional discontinuities, 1, Minimum variance errors, *J. Geophys. Res.*, *85*, 4695, 1980.

Lepping, R. P., and K. W. Behannon, Magnetic field directional discontinuities: Characteristics between 0.46 and 1.0 AU, *J. Geophys. Res.*, *91*, 8725, 1986.

Lin, Y., and L. C. Lee, Chaos and ion heating in a slow shock, *Geophys. Res. Lett.*, *18*, 1615, 1991.

Lin, Y., and L. C. Lee, Structure of the dayside reconnection layer in resistive MHD and hybrid models, *J. Geophys. Res.*, *98*, 3919, 1993.

Lin, Y., and L. C. Lee, Generation of region 1 and mantle field-aligned currents by the secondary rotational discontinuity, *Solar Wind Sources of Magnetospheric Ultra-*

Low-Frequency Waves, Geophys. Monogr. Ser., Vol. 81, edited by M. Engebreton, K. Takahashi, and M. Scholer, pp. 213-221, AGU, Washington D. C., 1994.

Lyu, L. H., and J. R. Kan, Nonlinear two-fluid hydromagnetic waves in the solar wind: Rotational discontinuity, soliton, and finite-extent Alfvén wave train solutions, J. Geophys. Res., 94, 6523, 1989.

Ma, Z. W., and L. C. Lee, A simulation study of generation of field-aligned currents and Alfvén waves by three-dimensional magnetic reconnection, J. Geophys. Res., 104, 10,177, 1999.

Medvedev, M. V., V. I. Shevchenko, P. H. Diamond, and V. L. Galinsky, Fluid models for kinetic effects on coherent nonlinear Alfvén waves, II, Numerical solutions, Phys. Plasmas, 4, 1257, 1997.

Neugebauer, M., The structure of rotational discontinuities, Geophys. Res. Lett., 16, 1261, 1989.

Neugebauer, M., Knowledge of coronal heating and solar wind acceleration obtained from observations of solar wind near 1 AU, in Solar Wind Seven, edited by E. Marsch and R. Schwenn, pp. 69-78, Pergamon, New York, 1992.

Neugebauer, M., D. R. Clay, B. E. Goldstein, B. T. Tsurutani, and R. D. Zwickl, A reexamination of rotational and tangential discontinuities in the solar wind, J. Geophys. Res., 89, 5393, 1984.

Parker, E. N., Heating solar coronal holes, Astrophys. J., 372, 719, 1991.

Richter, P., and M. Scholer, On the stability of rotational discontinuities, Geophys. Res. Lett., 16, 1257, 1989.

Richter, P., and M. Scholer, On the stability of rotational discontinuities with large phase angles, Adv. Space Res., 11(9), 111, 1991.

Rijnbeek, R. P., H. K. Biernat, M. F. Heyn, V. S. Semenov, C. J. Farrugia, D. J. Southwood, G. Paschmann, N. Sckopke, and C. T. Russell, The structure of the reconnection layer observed by ISEE 1 on 8 September 1978, Ann. Geophys., 7, 297, 1988.

Russell, C. T., P. Song, and R. P. Lepping, The Uranian magnetopause: Lessons from the Earth, Geophys. Res. Lett., 16, 1485, 1989.

Sakai, J.-I., and B. U. O. Sonnerup, Modulational instability of finite amplitude dispersive Alfvén waves, J. Geophys. Res., 88, 9069, 1983.

Scudder, J., Theoretical approaches to the description of magnetic merging: The need for finite, anisotropic ambipolar Hall MHD, Space Sci. Rev., 80, 235, 1997.

Sonnerup, B. U. O., and L. H. Cahill Jr., Explorer 12 observations of the magnetopause current layer, J. Geophys. Res., 73, 1757, 1968.

Sonnerup, B. U. O., and B. G. Ledley, Ogo 5 magnetopause structure and classical reconnection, J. Geophys. Res., 84, 399, 1979.

Sonnerup, B. U. O., G. Paschmann, I. Papamastorakis, N. Sckopke, G. Haerendel, S. J. Bame, J. R. Asbridge, J. T. Gosling, and C. T. Russell, Evidence for magnetic field reconnection at the Earth's magnetopause, J. Geophys. Res., 86, 10,049, 1981.

Su, S.-Y., and B. U. O. Sonnerup, First-order orbit theory of rotational discontinuities, Phys. Fluids, 11, 851, 1968.

Swift, D. W., and L. C. Lee, Rotational discontinuities and the structure of the magnetopause, J. Geophys. Res., 88, 111, 1983.

Tsurutani, B. T., and W. D. Gonzalez, The cause of high-intensity long-duration continuous AE activity (HILDCAAS): Interplanetary Alfvén wave trains, Planet. Space Sci., 35, 405, 1987.

Tsurutani, B. T., C. M. Ho, E. J. Smith, M. Neugebauer, B. E. Goldstein, A. Balogh, D. J. Southwood, and W. F. Feldman, The relationship between interplanetary discontinuities and Alfvén waves: Ulysses observations, Geophys. Res. Lett., 21, 2267, 1994.

Vasquez, B. J., and P. J. Cargill, A wave model interpretation of the evolution of rotational discontinuities, J. Geophys. Res., 98, 1277, 1993.

Vasquez, B. J., and J. V. Hollweg, Formation of arc-shaped Alfvén waves and rotational discontinuities from oblique linearly polarized wave trains, J. Geophys. Res., 101, 13,537, 1996.

Vasquez, B. J., and J. V. Hollweg, Formation of spherically polarized Alfvén waves and imbedded rotational discontinuities from a small number of entirely oblique waves, J. Geophys. Res., 103, 335, 1998a.

Vasquez, B. J., and J. V. Hollweg, Formation of imbedded rotational discontinuities with nearly field aligned normals, J. Geophys. Res., 103, 349, 1998b.

Wang, D. J., and B. U. O. Sonnerup, Electrostatic structure of the rotational discontinuity, II, Shock pair solutions, Phys. Fluids, 27, 2828 1984.

L. C. Lee, Department of Physics, National Cheng Kung University, Tainan, Taiwan.

Y. Lin, Physics Department, Auburn University, 206 Allison Laboratory, Auburn, AL 36849-5311. (e-mail: ylin@physics.auburn.edu)